INTERNATIONAL JOURNAL FOR INNOVATIVE RESEARCH IN MULTIDISCIPLINARY FIELD
ISSN(O): 2455-0620 [Impact Factor: 9.47]
Monthly, Peer-Reviewed, Refereed, Indexed Journal with IC Value : 86.87
Volume - 10, Issue - 9, September - 2024

DOIs:10.2015/IJIRMF/202409010 --:-- Research Paper / Article / Review

Numerical study of MHD convective heat transfer flow of Ethylene Glycol based SWCNT and MWCNT nanofluids in cylindrical annulus with variable viscosity, activation energy

M. Nagasasikala
Lecturer in Mathematics,
Government Degree College (A), Anantapuramu – 515 003, A.P., India
Email: mnagasasikala@gmail.com,

Abstract: *An investigation was performed to study the impact of variable electrical conductivity, viscosity on thermally radiating hydromagnetic flow of Ethyline Glycol based-Swcnt and MWcnt nanofluids in a concentric annular area in the presence of non-uniform heat sources. The nonlinear equations have been solved using the Galerkine finite element technique using quadratic polynomials. The velocity, temperature, and nano-concentration were investigated for various parametric values. It is observed that when the radiative heat flow (Rd) increases, so do the temperature and concentration.*

Key Words: *Varibale electrical conductivity, Viscosity, Non-Uniform heat sources Swcnt and Mwcnt-nanofluids, chemical reaction, thermal Radiation, Circular annulus, Soret effect.*

1. INTRODUCTION:

In many engineering systems, such as fuel cells, heat exchangers, and others, fluids play a crucial role in accelerating the rate of heat transfer. However, due to the weak heat conductivity of normal fluids, we need specialized, high-thermal conductivity fluids to solve this issue. Choi et.al. [13] proposed the term nanofluid for the first time. The major feature of nanofluids is that they have better thermal conductivity than ordinary fluids due to metallic nanometer-sized particles floating in fluid, which significantly contribute to thermal conductivity enhancement. Many researchers have concentrated their efforts on fluid flow and heat transfer topics, whether employing nanofluid or ordinary fluid. Materials like ethylene glycol, oils and water etc., having low conductivity are less impressive in heat conducting phenomenon. Thermal conductivity and heat transfer coefficient of base materials can be boosted through uinclusion of nanoparticles (Choi and Eastman [12]; Buongiorno [11]. Gopi [15] and Srijana Sharma and Prasada Rao[32] have extended this work to include theeffect of heat generating sources on hydromagnetic convective heat transfer flow of rotating Swcnt and Mwcnt nanofluids in a vertical channel with inconstant viscosity. Recently Lalramngaihzualí and Prasada Rao [22] were extended the work of numerical study of MHD convective heat transfer flow of Ethylene Glycol based SWCNT and MWCNT nanofluids in cylindrical annulus with variable viscosity, activation energy.

Because of its high electrical conductivity, which varies with temperature and metal, the velocity field and distribution of heat of liquid metals are altered in the presence of a transverse magnetic field that changes in inverse proportion to temperature. As a result, one of the most effective methods for improving heat transport is to use an electric field. As a result, current research focuses on temperature-dependent electrical conductivity. However, we want to know whether controlled by temperature electrical conductivity has a substantial impact on the flow and fluid characteristics of two vertical plates.The Simulation of revised nanofluid model in the stagnation region of cross fluid by expanding–contracting cylinder were investigated by Waqas[38]. The Thermally radiative stagnation point flow of Maxwell nanofluid due to unsteady convectively heated stretched surface was investigated by Hayat et al[16]. Entropy optimized Darcy–Forchheimer nanofluid (silicon dioxide, molybdenum disulfide) subject to temperature dependent viscosity were investigated by Abbas [1]. Engineers can control much metallurgical process by taking suitable electrical conductivity of fluids. Jewel Rana et al [17] have investigated effect of variable conductivity on MHD free convection flow past an exponential accelerated inclined plate.

Reinforcing warming or bracing in an industrial process can save energy, reduce growth time, raise heated rating, and extend equipment life. Increased thermal energy transfer has a qualitative effect on several processes. The development of high-performance thermal systems for heat transfer enrichment has recently gained popularity. Single-walled carbon nanotubes (SWCNTs), a member of the carbon family, are one-dimensional equivalents of zero-dimensional falling molecules with unusual structural and electrical characteristics. Single-walled nanotubes are the most likely choice for miniaturizing electronics beyond the microelectrothermal scale now used in electronics. Carbon nanotubes (CNTs) have received a lot of interest because to their linear model and significant mechanical, thermal, and electrical properties (Al-Marri et al. [7], Arash Karimipour et. Al. [9], Maria Imtiaz et al. [25], Mehdi Nojoomizadeh and Arash Karimipour [26], Shahsavar et al. [31]). The study for thermophysical properties of CNTs nanofluids with base fluid as mixture of water and ethylene glycol has been presented by Kumaresan and Velraj [21]. And this study noted that the maximum thermal conductivity enhances up to 19.75% for the nanofluid containing 0.45 vol.% MWCNT at 40°C. The entropy generation Berrehal [10], Shafiq et al [30], Vijayalakshmi [37], Kamali and Binesh [18] CNT'S are rolled–up grapheme sheets arranged in a cylindrical shape. They are of two types single walled (SWCNT's) and multi-walled (MWCNT's). Kiran Kumar et.al.[20] have described the effect of thermal radiation on nonDarcy hydromagnetic convective heat and mass transfer flow of a water -SWCNT's and MWCNT's nanofluids in a cylindrical annulus with thermo-diffusion and chemical reaction.

In chemistry and physics, activation energy is the minimum amount of energy that must be provided for compounds to result in a chemical reaction. The activation energy (*E*a) of a reaction is measured in joules per mole (J/mol), kilojoules per mole (kJ/mol) or kilocalories per mole (kcal/mol). Activation energy can be thought of as the magnitude of the potential barrier (sometimes called the energy barrier) separating minima of the potential energy surface pertaining to the initial and final thermodynamic state. For a chemical reaction to proceed at a reasonable rate, the temperature of the system should be high enough such that there exists an appreciable number of molecules with translational energy equal to or greater than the activation energy. The term "activation energy" was introduced in 1889 by the Swedish scientist Svante Arrhenius.[34]. The Natural convection of the nanofluid in a concentric annulus with variable viscosity and thermal conductivity with activation energy on flow phenomenon are studied by several authors AbuNada et al.[2] and Abu-Nada[3], Amotosh Tiwari et al [8], Kathyani and Subramanyam[19], Satya Narayana and Ramakrishna[29], Nagasasikala [27], Devasena [14]. For example, Adesanya et al. [5] investigated the heat resistance of a reactive third-grade fluid flowing through a porous material. The stability of a one-step exothermic reaction was thoroughly investigated in Makinde [24]. Lebelo et al. [23] investigated the heat stability of radiative and convective reacting fluids in a combustible slab. Furthermore, Furthermore, Adebowale Martins Obalalu et al [4] and Adeshina et al [6] have added on the findings of Impact of variable conductivity of energy on the stability of heat of the MHD reactive squeezed fluid flow through a channel using a spectral collocation approach and flow between two vertical plates in a mixture of Arrhenius energy and exothermic chemical reaction. The purpose of this analysis is to examine and emphasise the influence of thermal radiation and heat source on the transfer of heat through convection flow of Swcnt-Eg and Mwcnt-Eg nanofluids in a concentric annulus. This is accomplished by applying a theoretical mathematical model first developed by Tiwari and Das [36]. Their model demonstrated how the volume percentage of nanoparticles influences the viscosity of the nanofluid.The behaviour of velocity, temperature, and nanoconcentration is investigated at various axial locations. Variations in the governing parameters were used to calculate shear stress as well as the rate of heat and mass transfer.

2. FORMULATION OF THE PROBLEM:

We analyse the mixed convective flow of a SWCNt-Egr and Mwcnt-Eg nanofluids in a vertical circular annulus through a porous medium whose walls are maintained at a constant heat and concentration. The flow, temperature and concentration in the fluid are assumed to be fully developed. Both the fluid and porous region have constant physical properties and the flow is a mixed convection flow taking place under thermal and molecular buoyancies and uniform axial pressure gradient. The Boussinesq approximation is invoked so that the density variation is confined to the thermal and molecular buoyancy forces. The Brinkman-Forchheimer-Extended Darcy model which accounts for the inertia and boundary effects has been used for the momentum equation in the porous region. The momentum, energy and diffusion equations are coupled and non-linear. Also the flow is unidirectional along the axial direction of the cylindrical annulus. Making use of the above assumptions the governing equations are

$$-\frac{\partial p}{\partial z}+\frac{1}{\rho_{nf}\delta r}\frac{\partial}{\partial r}\left((\mu_{nf}(T)\,\mathrm{r}\frac{\partial u}{\partial r})\right)-(\frac{\mu_{nf}}{\rho_{nf}k})u-\frac{\sigma_f(T,C)\mu_e^2H_0^2}{\rho_{nf}r^2}-\frac{\delta F}{\rho_{nf}\sqrt{k}}u^2+(\rho\beta)_{nf}(T-T_o)=0 \qquad (2.1)$$

$$(\rho C_p)_{nf}\, u\frac{\partial T}{\partial z} = k_{nf}\left(\frac{\partial^2 T}{\partial r^2}+\frac{1}{r}\frac{\partial T}{\partial r}\right)+q'''-\frac{1}{r}\frac{\partial (rq_r)}{\partial r}+Q_1^{'}(C-C_0) \quad (2.2)$$

$$u\frac{\partial C}{\partial z} = D_B\left(\frac{\partial^2 C}{\partial r^2}+\frac{1}{r}\frac{\partial C}{\partial r}\right)-k_c^{'}C+\frac{D_m K_T}{T_s}\left(\frac{\partial^2 T}{\partial r^2}+\frac{1}{r}\frac{\partial T}{\partial r}\right)- \quad (2.3)$$

$$-kc(\mathrm{C}-\mathrm{C}_0)\left(\frac{T}{T_o}\right)^n Exp\left(-\frac{E_a}{KT}\right)$$

where u is the axial velocity in the porous region, T , C are the temperature and concentration of the fluid, k is the permeability of porous medium, k_f is the thermal diffusivity, F is a function that depends on Reynolds number, the microstructure of the porous medium and D_B is the molecular diffusivity, D_m is the mass diffusivity, K_T mass diffusion ratio, β is the coefficient of the thermal expansion, q_R is the radiation absorption coefficient, Cp is the specific heat, ρ is density ,g is gravity, ρ_{nf} is the effective density . μ_{nf} is the effective dynamic viscosity, k_{nf} is the thermal conductivity of the nanofluid.

The dynamic viscosity of the nanofluids is assumed to be temperature dependent as follows:

$$\mu_{nf}(T) = \mu_f Exp(-m(T-T_2)) \quad (2.9)$$

where μ_{nf} is the nanofluid viscosity at the ambient temperature To, m is the viscosity variation parameter which depends on the particular fluid.

The relevant boundary conditions are

$u = 0$, $T=T_w$, $C=C_w$ at r = a&a+s (2.4)

Following Tao [22], we assume that the temperature and concentration of the both walls is $T_w = T_0 + Az$, $C_w = C_0 + Bz$ where A and B are the vertical temperature and concentration gradients which are positive for buoyancy –aided flow and negative for buoyancy – opposed flow, respectively, T_0 and C_0 are the upstream reference wall temperature and concentration ,respectively.

The coefficient q''' is the rate of internal heat generation (>0) or absorption(<0). The internal heat generation /absorption q''' is modelled as

$$q''' = \left(\frac{k_f}{a^2 v}\right)(A^{\bullet}(T_w - T_0)u + B^{\bullet}(T-T_0)) \quad (2.5)$$

where $A^{\bullet}$ and $B^{\bullet}$ are coefficients of space dependent and temperature dependent internal heat generation or absorption respectively. It is noted that the case $A^{\bullet}$>0 and $B^{\bullet}$>0, corresponds to internal heat generation and that $A^{\bullet}$ <0 and $B^{\bullet}$<0, the case corresponds to internal heat absorption case.

We now define the following non-dimensional variables for the fully developed laminar flow in the presences of radial magnetic field, the velocity depend only on the radial coordinate and all the other physical variables except temperature, concentration and pressure are functions of r and z, z being the vertical co-ordinate .The temperature and concentration inside the fluid can be written as

$$T = T^{\bullet}(r) + Az \quad , \quad C = C^{\bullet}(r) + Bz \quad (2.6)$$

The effective density of the nanofluid is given by

$$\rho_{nf} = (1-\varphi)\rho_f + \varphi\rho_s \quad (2.7)$$

Where ϕ is the solid volume fraction of nanoparticles. Thermal diffusivity of the nanofluid is

$$\alpha_{nf} = \frac{k_{nf}}{(\rho C_p)_{nf}} \quad (2.8)$$

Where the heat capacitance C_p of the nanofluid is obtained as

$$(\rho C_p)_{nf} = (1-\varphi)(\rho C_p)_f + \varphi(\rho C_p)_s \quad (2.9)$$

And the thermal conductivity of the nanofluid k_{nf} for spherical nanoparticles can be written as

$$\frac{k_{nf}}{k_f} = \frac{(k_s + 2k_f) - 2\phi(k_f - k_s)}{(k_s + 2k_f) + \phi(k_f - k_s)} \tag{2.10}$$

The thermal expansion coefficient of nanofluid can determine by

$$(\rho\beta)_{nf} = (1-\varphi)(\rho\beta)_f + \varphi(\rho\beta)_s \tag{2.11}$$

Also the effective dynamic viscosity of the nanofluid given by

$$\mu_{nf} = \frac{\mu_f}{(1-\varphi)^{2.5}}, \quad \sigma_{nf} = \sigma_f\left(1 + \frac{3(\sigma-1)\phi}{\sigma + 2 - (\sigma-1)\phi}\right), \sigma = \frac{\sigma_s}{\sigma_f} \tag{2.12}$$

Where the subscripts nf, f and s represent the thermo physical properties of the nanofluid, base fluid and the nanosolid particles respectively and ϕ is the solid volume fraction of the nanoparticles. The thermo physical properties of the nanofluid are given in Table 2.1.

The thermo physical properties of the nanofluids are given in Table 1 (See Oztop and Abu-Nada [28]).

Table – 2.1

Physical properties	Fluid phase (Eg)	**Swcnt's**	**Mwcnt's**
C_p(j/kg K)	**1115**	**425**	**796**
ρ(kg m^3)	2430	**2600**	**1600**
k(W/m K)	0.253	**6600**	**3000**
βx10^{-5} 1/k)	5.7	2.0	**2.0**
σ	**10.7**	**10^6**	**10^7**

We now define the following non-dimensional variables

$$z^* = \frac{z}{a} \quad , \quad r^* = \frac{r}{a} \quad , \quad u^* = (\frac{a}{\nu})u \ , \ p^* = \frac{pa\delta}{\rho\nu^2} \ ,$$

$$\theta^*(r^\bullet) = \frac{T^\bullet - T_0}{P_1 Aa} \quad , \quad C^*(r^\bullet) = \frac{C^\bullet - C_0}{P_1 Ba} \ , \ s^* = \frac{s}{a}, P_1 = \frac{dp}{dx} \tag{2.13}$$

Introducing these non-dimensional variables, the governing equations in the non-dimensional form are (on removing the stars)

$$(\frac{\partial^2 u}{\partial r^2} + \frac{1}{r}\frac{\partial u}{\partial r} - \mathrm{B}(\frac{\partial u}{\partial r})(\frac{\partial T}{\partial r})) = A_1 A_3 \, \mathrm{e}^{B\theta} + \delta A_1 (D^{-1} + \frac{A_6 M^2 (1 + \varepsilon\theta + \beta_1 \mathrm{C})\, \mathrm{e}^{B\theta}}{r^2})u + \delta A_1 A_4 G \, \mathrm{e}^{B\theta}(\theta) \tag{2.14}$$

$$A_2(1 + \frac{4Rd}{3})(\frac{\partial^2\theta}{\partial r^2} + \frac{1}{r}\frac{\partial\theta}{\partial r}) + (A_{11}u + B_{11}\theta) + Q_1 C = A_5 \, \mathrm{Pr}\, u \tag{2.15}$$

$$(\frac{\partial^2 C}{\partial r^2} + \frac{1}{r}\frac{\partial C}{\partial r}) - \gamma C = Sc\, u + ScSr\left(\frac{\partial^2\theta}{\partial r^2} + \frac{1}{r}\frac{\partial\theta}{\partial r}\right) - \gamma C(1 + n\delta\theta)Exp(-\frac{E_1}{1+\delta\theta}) \tag{2.16}$$

where

$B = m(T_0 - T_i)$ (Viscosity parameter)

$\Delta = FD^{-1/2}$ (Inertia parameter or Forchheimer number)

$G = \frac{g\beta(T_e - T_i)a^3}{\nu^2}$ (Grashof number), $M^2 = \frac{\sigma\mu_e^2 H_0^2}{a\nu}$ (magnetic parameter), $D^{-1} = \frac{a^2}{k}$ (Inverse Darcy parameter), $P_r = \frac{\mu C_p}{k_f}$ (Prandtl number), $Rd = \frac{4\sigma^\bullet T_o^3}{k_f \beta_R}$ (Thermal radiation parameter), $Sc = \frac{\nu}{D_B}$ (Schmidt number), $\gamma = \frac{k_c a^2}{D_B}$ (Chemical Reaction parameter), $So = \frac{D_m K_T (T_0 - T_{i)}}{T_s(C_0 - C_i)}$ (Soret parameter), $Q_1 = \frac{Q_1^{'}(C_w - C_0)}{a^2(T_w - T_0)}$

(Radiation absorption parameter), $\theta_w = \frac{T}{T_o}$, $\delta = \theta_w - 1$, Temperature difference ratio, $E_1 = \frac{E_a}{KT_0}$ (Activation energy parameter)

$$A_1 = \frac{1}{(1-\varphi)^{2.5}}\ , A_2 = (1-\varphi) + \varphi(\frac{\rho_s}{\rho_f})\ A_1 = \frac{1}{(1-\varphi)^{2.5}}\ \ , A_2 = (1-\varphi) + \varphi(\frac{\rho_s}{\rho_f})\ ,\ A_3 = 1-\varphi+\varphi\frac{(\rho C_p)_s}{(\rho C_p)_f}\ ,$$

$$A_4 = 1-\varphi+\varphi(\frac{(\rho\beta)_s}{(\rho\beta)_f}\ ,\quad A_5 = \frac{k_{nf}}{k_f}\quad A_6 = (1+\frac{3(\sigma-1)}{\sigma+2-(\sigma-1)\phi}\ ), \sigma_{nf} = \sigma_f A_6,\ \sigma = \frac{\sigma_s}{\sigma_f}$$

The corresponding non-dimensional conditions are

$u = 0 \quad \theta = 0$ C=0 at r=1 and 1+s (2.17)

3. METHOD OF SOLUTION (Finite Element Analysis):

The finite element analysis with quadratic polynomial approximation functions is carried out along the radial distance across the circular duct. The behavior of the velocity, temperature and concentration profiles has been discussed computationally for different variations in governing parameters. The Galerkin method has been adopted in the variational formulation in each element to obtain the global coupled matrices for the velocity, temperature and concentration in course of the finite element analysis.

Choose an arbitrary element e_k and let u^k, θ^k and C^k be the values of u, θ and C in the element e_k. We define the error residuals as

$$E_p^k = \frac{d}{dr}\left(r\frac{du^k}{dr}\right) - B(\frac{du^k}{dr})(\frac{d\theta^k}{dr}) + \delta A_1 A_4 rG\,e^{B\theta^k}(\theta^k) - \delta A_1(D^{-1} + \frac{A_6 M^2(1+\varepsilon\theta+\beta_1 C)e^{B\theta^k}}{r^2})ru^k - A_1 A_3 e^{B\theta^k} \quad (3.1)$$

$$E^k{}_\theta = \frac{A_2}{\Pr}(1+\frac{4Rd}{3})\frac{d}{dr}\left(r\frac{d\theta^k}{dr}\right) - A_5 ru^k + (A_{11}u^k + B_{11}\theta^k) + Q_1 C^k \quad (3.2)$$

$$E^k{}_c = \frac{d}{dr}\left(r\frac{dC^k}{dr}\right) - rScu^k - \gamma C^k + ScS_r\frac{d}{dr}\left(r\frac{d\theta^k}{dr}\right) - \gamma C^k(1+n\delta\theta^k)Exp(-\frac{E_1}{1+\delta\theta^k}) \quad (3.3)$$

where u^k, θ^k & C^k are values of u, θ& C in the arbitrary element e_k. These are expressed as linear combinations in terms of respective local nodal values.

$$u^k = u_1^k\psi_1^k + u_2^k\psi_1^k + u_3^k\psi_3^k\ ,\quad \theta^k = \theta_1^k\psi_1^k + \theta_2^k\psi_2^k + \theta_3^k\psi_3^k,\ C^k = C_1^k\psi_1^k + C_2^k\psi_2^k + C_3^k\psi_3^k$$

where ψ_1^k, ψ_2^k --------- etc are Lagrange's quadratic polynomials.

Galarkin's method is used to convert the partial differential Equations (3.1) – (3.3) into matrix form of equations which results into 3x3 local stiffness matrices. All these local matrices are assembled in a global matrix by substituting the global nodal values and using inter element continuity and equilibrium conditions. The resulting global matrices have solved by iterative procedure until the convergence i.e $|u_{i+1}-u_i|<10^{-6}$ is obtained.

4. SHEAR STRESS,NUSSELT NUMBER AND SHERWOOD NUMBER

The shear stress (τ) is evaluated using the formula $\tau = (\frac{du}{dr})_{r=1,1+s}$.

The rate of heat transfer (Nusselt number) is evaluated using the formula $Nu = -(\frac{d\theta}{dr})_{r=1,1+s}$.

The rate of mass transfer (Sherwood number) is evaluated using the formula $Sh = -(\frac{dC}{dr})_{r=1,1+s}$

5. COMPARISON:

In the absence of activation energy (E1=0) & variable viscosity (B=0) .The results are good agree with Kiran Kumar et.al.[20]

Table – 5.1

Parameter		Kiran Kumar et.al.[20] results		Present Results		Kiran Kumar et.al.[20] results		Present Results	
		Eg-Swcnt				Eg-Mwcnt			
		τ(1)	Nu(1)	τ(1)	Nu(1)	τ(1)	Nu(1)	τ(1)	Nu(1)
Rd	0.5	-0.167074	0.999968	-0.502712	-0.184469	-0.102191	0.999955	-0.502928	-0.405918
	1.5	-0.167076	0.999993	-0.502714	-0.102477	-0.102193	0.999975	-0.502929	-0.225483
	3.5	-0.167084	0.999996	-0.502716	-0.040093	-0.102194	0.999987	-0.502930	-0.088787
	5.0	-0.167165	0.999997	-0.502718	-0.020087	-0.102195	0.999999	-0.503000	-0.066888
Ec	0.01	-0.334342	0.999954	-0.502712	-0.184469	-0.102191	0.999955	-0.502928	-0.405918
	0.03	-0.167074	0.999965	-0.502706	-0.304786	-0.102190	0.999951	-0.502914	-0.670669
	0.05	-0.011655	0.999975	-0.502697	-0.425090	-0.102188	0.999947	-0.502892	-0.943638
	0.07	-0.010458	0.999976	-0.502588	-0.518722	-0.102179	0.999942	-0.502688	-1.08298
ϕ	0.05	-0.167074	0.999968	-0.502712	-0.184469	-0.460268	0.999883	-0.502928	-0.405918
	0.10	-0.198163	0.999966	-0.503538	-0.185328	-0.460244	0.999879	-0.503973	-0.407908
	0.15	-0.244968	0.999963	-0.504146	-0.186028	-0.464207	0.999877	-0.504802	-0.412275
	0.20	-0.300647	0.999958	-0.505064	-0.187215	-0.470861	0.999873	-0.505176	-0.421433

6. GRAPHICAL ANALYSIS:

The equations governing the flow,heat and mass transfer flow Ethylene Glycol based SWCNT and MWCNT nanofluids have been solved by employing Galerkine kinite element analysis with quadratic interpolation polynomials.We have chosen here Pr=6.2 while Rd, Ec, B, E1, A11, B11,δ,ε and β_1 are varied over a range, which are listed in the Figure legends.

In this analysis, we explore the combined influence of Variable electrical conductivity/heat sources / activation energy/Thermal radiation/variable viscosity on hydromagnetic convective heat transfer flow of Ethylene Glycol based SWCNT and MWCNT nanofluids through a porous medium in a vertical channel. The resulting non-linear,coupled equations have been solved by finite element measure with quadratic interpolation functions. The velocity, temperature and nano-concentration are exhibited for different parametric variation in figs. 6.1 - 6.10. The skin fraction, Nusselt and Sherwood numbers on the wall have been evaluated numerically.

Figs. 6.1(a)-6.1(c) represent the variation of the flow variables (u,θ,C) with variable viscosity parameter 'B'. From the profiles we find that for higher values of viscosity parameter (B), we notice a depreciation in (u,θ,C) in all the nanofluids.This may be due to the fact that with increase in 'B' the momentum, thermal and solutal boundary layers becomes thinner. The values of (u,θ,C) in Eg-SWCNT case are relatively higher than those in Eg-MWCNT case. The effect of thermal radiation on (u,θ,C) can be absorbed from figs. 6.2(a)-6.2(c) fixing the other parameters. From figure 6.2(a) & 6.2(c) we find that magnitude of velocity and nanoconcentration (C) grow with higher values of radiation parameter (Rd) while the temperature experiences reduction with 'Rd'. The may be attributed to the fact that momentum and solutal boundary layers become thicker and thermal boundary layer becomes thinner with rising values of 'Rd'. From the figures we also find that the values of flow variables (u,θ,C) in Eg-SWCNT case are relatively smaller than those in Eg-MWCNT case.

Figs. 6.3(a)-6.3(c) demonstrate the influence of viscosity dissipation (Ec) on (u,θ,C). Higher the dissipative energy smaller the magnitude of velocity and nanoconcentration and larger the temperature distribution in the flow region. This may be due to the fact that the momentum , solutal boundary layers become thinner and thermal boundary layer becomes thicker with increased values of 'Ec'.The values of velocity and concentration in Eg-SWCNT case are relatively greater than those in Eg-MWCNT case while an opposite effect is observed in the case of temperature.

Figs. 6.4(a)-6.4(c)/figs. 6.5(a)-6.5(c) represent variation of (u,θ,C) / temperature dependent heat sources.The velocity, temperature, nanoconcentration experienced the depreciation with rising values of A11/B11. The momentum thermal and boundary layer becomes thinner with larger values of A11/B11. It is noted that, owing to the presence of heat generation or source(Q>0),the thermal state of the fluid increases .Therefore the fluid temperature increases within the boundary layer.Also we notice that the values of velocity temperature nanoconcentration in Eg-SWCNT case are relatively higher than those in Eg-MWCNT case.

Figs. 6.6(a)-6.6(c) exhibited the influence of activation energy parameter (E1). From the profiles we find that the velocity and temperature reduces and concentration enhances with higher values of 'E1'. This may be due to the fact that the momentum and thermal boundary layer becomes thinner while solutal boundary layer becomes thicker with the increased in values of E1. The values of u and θ in SWCNT case are relatively smaller than those in MWCNT case, while an opposite effect is observed in the behaviour of nanoconcentration.

Figs. 6.7(a)-6.7(c) represent (u,θ,C) with temperature difference ratio (δ) . The velocity and concentration depreciates with 'δ' in both types of nanofluids while the temperature reduces in SWCNT case and enhances in MWCNT case. The values of u & C in SWCNT nanofluid are relatively greater than those in Eg-SWCNT nanofluid.

Figs.6.8a-6.8c and 6.9a-6.9c demonstrate the effect of temperature and concentration dependent electrical conductivity(ε, β1on flow variables.From the profiles it is noticed that increasing values of temperature dependent electrical conductivity(ε) leads to enhancement in nanofluid velocity,temnperature and concentration in the boundary layer.This is owing to the fact that the momentum.thermal and solutal boundary layers become thinner with higher values of ε, The values of temperature and nanoconcentration in SWCNT are relatively smaller than those in MWCNT nanofluid while opposite behaviour is observed in the nature of temperature(figs.6.9a-6.9c). Enhanced values of nanoconcentration dependent electrical conductivity (β1) give rise to depreciation in velocity, temperature and concentration in the boundary layer. Also the values of u,θ and C in SWCNT nanofluid are greater than those in MWCNT nanofluid with rising values of β1.

Figs.6.10a-6.10c exhibit the variation of velocity,temperature and nanoconcentration with radiation absorption parameter(Q1).From the profiles it is noted that higher the radiation absorption parameter(Q1)thinner the momentum ,thermal and solutal boundary layers,as consequence the velocity,temperature and nanoconcentration experience enhancement in the boundary layer in both types of nanofluids.Ftom the profiles it is noticed that,the values of velocity and nanoconcentration in Eg-SWCNT nanofluid are relatively greater than those in Eg based MWCNT nanofluid while opposite behaviour is observed in nanofluid temperature in te boundary layer(figs.6.10a-6.10c).

The shear stress (τ) at the inner and outer cylinder (r =1,2) have been shown in table 6.1 of different variations of Rd, Ec, A11, B11,E1, δ,ε and β1 .From the tabular values it is found that the stress decays at both the cylinders with increased values of viscosity parameter(B)/ Eckert number (Ec) / space and temperature dependent heat source (A11,B11)/activation energy parameter(E1)/ temperature difference ratio (δ).An increase in radiation parameter(Rd) enhances at the inner cylinder while it reduces at the outer cylinder in both types of nanofluids.The shear stress decays at both the cylinders in SWCNT nanofluid while it augments at r=1 and 2 in MWCNT nanofluid with rising values of temperature dependent electrical conductivity(ε) .It grows on both the cylinders with increase in nanoconcentration dependent electrical conductivity(β1) in both Eg based SWCNT and MWCNT nanofluids.Higher the radiation absorption parameter(Q1) smaller the satress at the inner cylinder r=1 and larger at the outer cylinder r=2. From the above analysis, we find that the shear stress at inner cylinder (r = 1) in Eg-SWCNT nanofluid are relatively lesser than those in Eg-MWCNT case,while an opposite effect is observed in the behaviour of (τ) at the outer cylinder (r = 2).

The local rate of heat transfer (Nusselt number) at the inner and outer cylinder (r = 1,2) have been shown in table 6.2 for different parametric variations.From the tabular values, it is found that the Nusselt number reduces on both cylinders (r = 1and 2)) with increase in viscosity parameter(B)/ radiation parameter (Rd)/ space asnd temperature dependent heat sourcepatrameters (A11,B11)/ radiation absorption parameter(Q1)/Activation energy partameter(E1)/nanoconcentratrion dependent electrical conductivity parameter(β1) in both typs of Eg based SWCNT and MWCNT nanofluids. Higher the dissipation (Ec) larger the rate of heat transferNu) at r=1 and 2 in both types of nanofluids. Increaqse in temperature dependent electrical conductivity(ε)reduces Nu at r=1 and 2 in Eg based SWCNT nanofluiud while in Eg based M WCNT nanofluid,Nu grows at both the cylinders.Increase in temperature difference ratio(δ)decays Nu at r=1 and 2 in Eg basaed SWCNT nanofluid while in Eg based MWCNT nanofluid.Nu decays at r=1 and enhances at r=2.From the above analysis it is noted that the values of Nusselt number at both the cylinders in Eg-SWCNT nanofluid are relatively lesser than those in Eg-MWCNT nanofluid with increaqse in B/A11/B11/Rd/Ec/Ec/E1/δ,while reversed effect is observed in Nu with larger values of Q1,ε and β1.

The local rate of mass transfer (Sherwood number) is presented in table 6.3 for different values of E1/δ/B/Rd/Ec/ε/β/A11/B11. From the tabular values it is found that increase in viscocity parameter(B)/Eckert number(Ec)/temperature difference ratio(δ)/Space and temperature dependent heat source parameter(A11,B11) small;er the rate of mass transfer at δ=1 and 2 in both Eg based SWCNT and MWCNT nanofluids.The Sherwood number(Sh) experiences augmentation with rising values of rd and activation energy parameter(E1) at δ=1 and 2 in both types of nanofluids.From the above analysis we find that the values of rate of mass transfer at both cylinder (r = 1,2) in Eg-SWCNT nanofluid are relatively higher than those in Eg-MWCNT case.

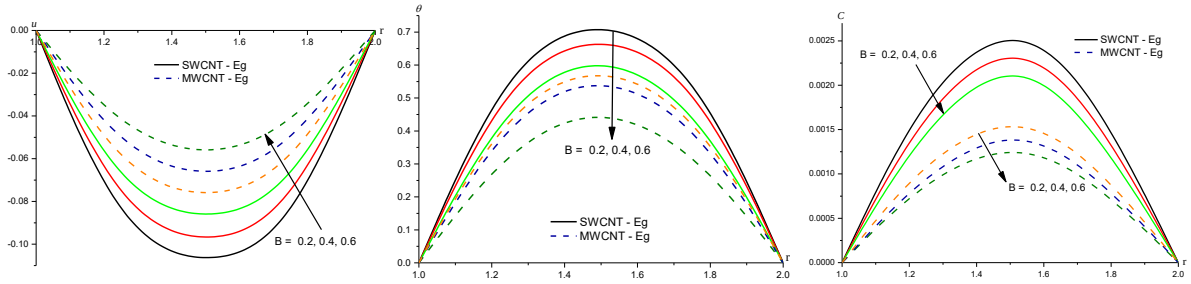

Fig.6.1 : Variation of [a] Velocity (*u*), [b] Temperature(θ), [c] Nanoconcentration(C) with B
Rd=0.5, Ec=0.1, E1=0.1, δ=0.1, ε=0.1, β1=0.15, Q1=0.25, A11=0.2,B11=0.3,

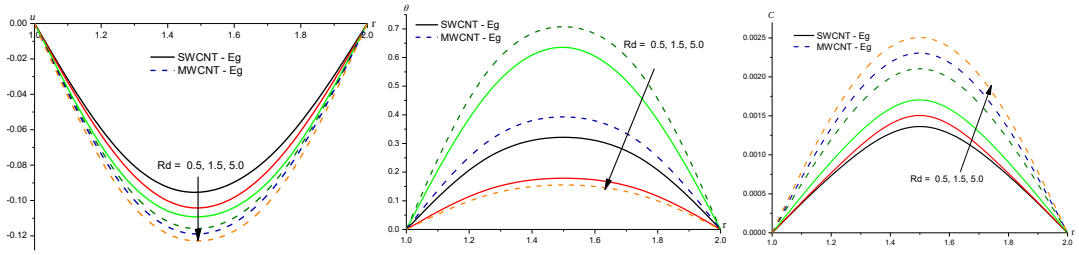

Fig.6.2 : Variation of [a] Velocity (*u*), [b] Temperature(θ), [c] Nanoconcentration(C) with Rd
Ec=0.1, A11=0.1, B11=0.5, B=0.2, E1=0.1, δ=0.1, ε=0.1, β1=0.15, Q1=0.25, A11=0.2,B11=0.3,

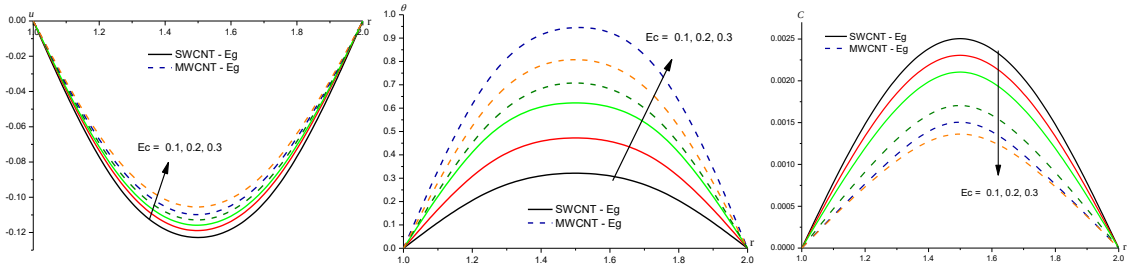

Fig.6.3 : Variation of [a] Velocity (*u*), [b] Temperature(θ), [c] Nanoconcentration(C) with Ec
Rd=0.5, B=0.2, E1=0.1, δ=0.1, ε=0.1, β1=0.15, Q1=0.25, A11=0.2,B11=0.3,

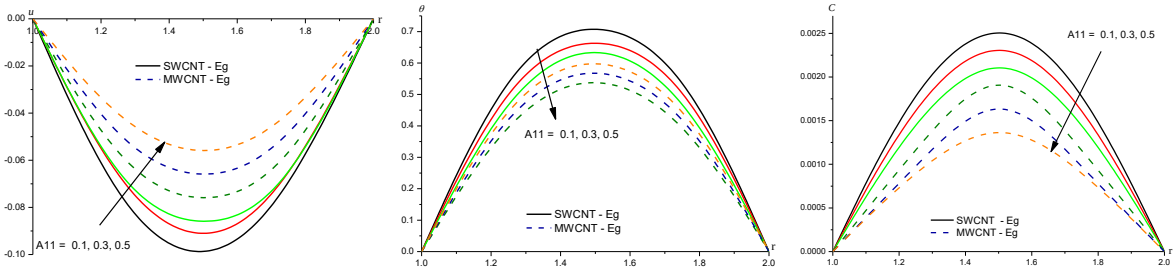

Fig.6.4 : Variation of [a] Velocity (*u*), [b] Temperature(θ), [c] Nanoconcentration(C) with A11
Rd=0.5, Ec=0.1, B=0.2, E1=0.1, ε=0.2, β1=0.15, Q1=0.25

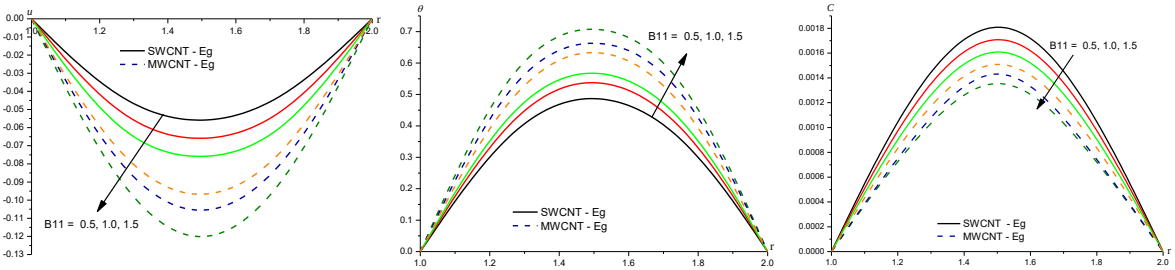

Fig.6.5 : Variation of [a] Velocity (*u*), [b] Temperature(θ), [c] Nanoconcentration(C) with B11
Rd=0.5, Ec=0.1, B=0.2, E1=0.1, ε=0.2, β1=0.15, Q1=0.25

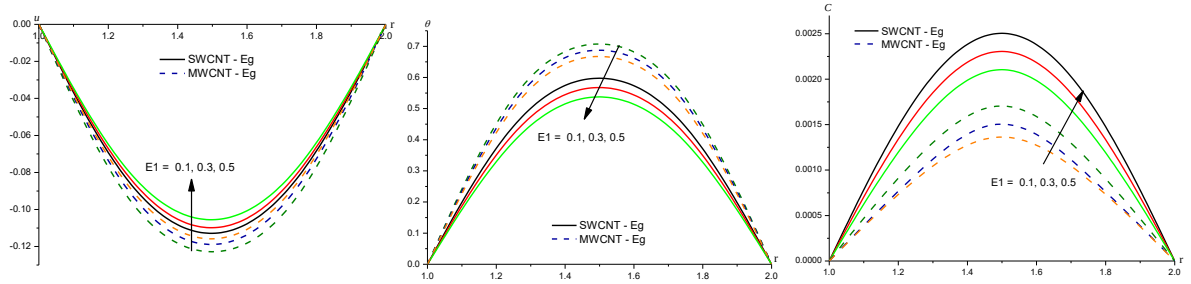

Fig.6.6 : Variation of [a] Velocity (*u*), [b] Temperature(θ), [c] Nanoconcentration(C) with E1
Rd=0.5, Ec=0.1, A11=0.1, B11=0.5, B=0.2, δ=0.1, ε=0.1, β1=0.15, Q1=0.25, A11=0.2,B11=0.3,

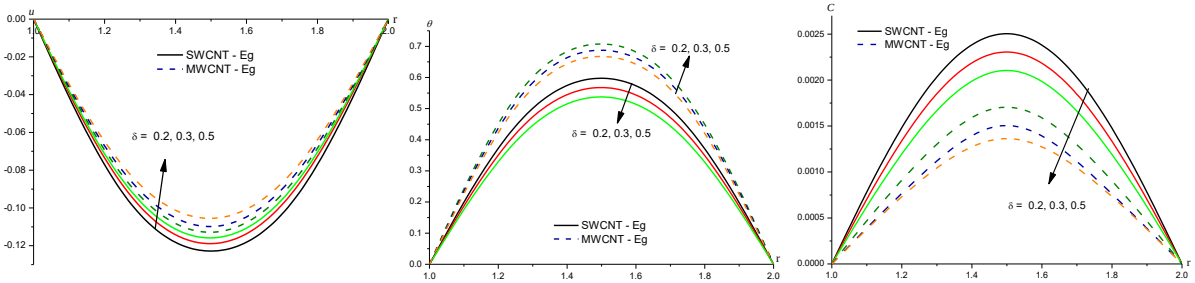

Fig.6.7 : Variation of [a] Velocity (*u*), [b] Temperature(θ), [c] Nanoconcentration(C) with δ
Rd=0.5, Ec=0.1, B=0.2, E1=0.1, ε=0.1, β1=0.15, Q1=0.25, Q=2

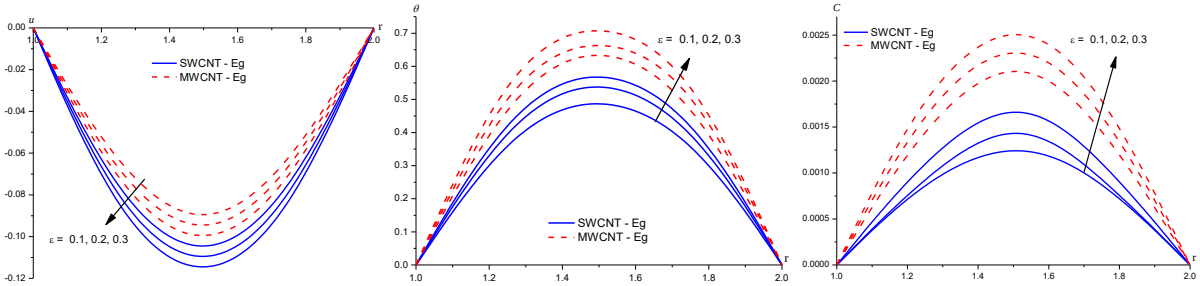

Fig.6.8 : Variation of [a] Velocity (*u*), [b] Temperature(θ), [c] Nanoconcentration(C) with ε
Rd=0.5, Ec=0.1, B=0.2, E1=0.1, β1=0.15, Q1=0.25, A11=0.2,B11=0.3,

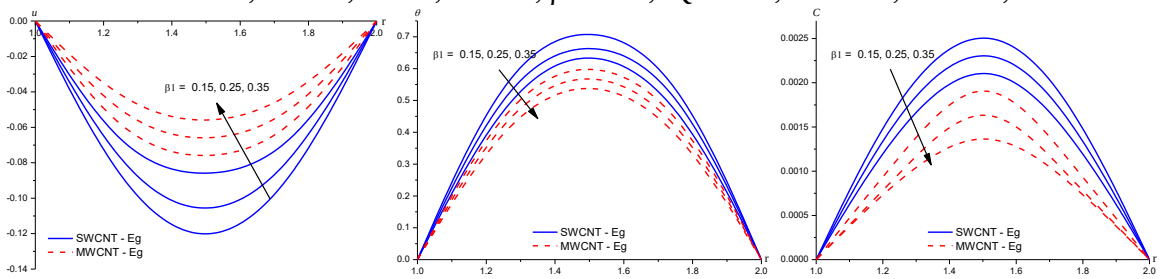

Fig.6.9 : Variation of [a] Velocity (*u*), [b] Temperature(θ), [c] Nanoconcentration(C) with β1
Rd=0.5, Ec=0.1, B=0.2, E1=0.1, ε=0.2, Q1=0.25, A11=0.2,B11=0.3,

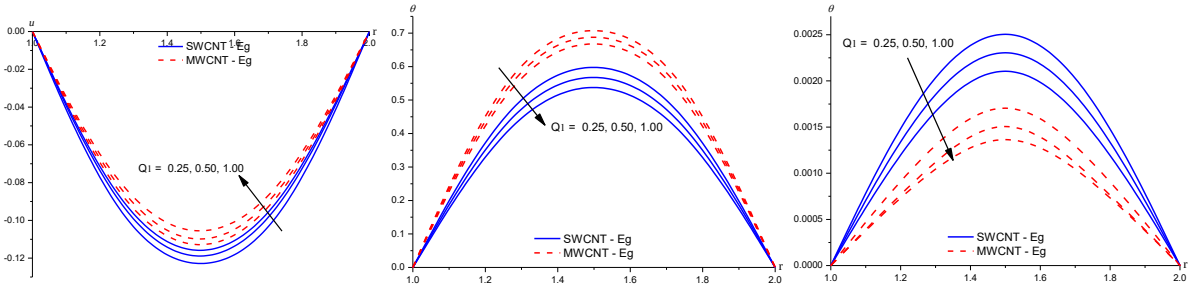

Fig.6.10 : Variation of [a] Velocity (*u*), [b] Temperature(θ), [c] Nanoconcentration(C) with Q1
Rd=0.5, Ec=0.1, B=0.2, E1=0.1, ε=0.2, β1=0.15, A11=0.2,B11=0.3,

Table 6.1 : Skin friction(τ) & Nusselt number(Nu) with Swcnt-Eg and Mwcnt-Eg at r=1

Paramater		Eg-Swcnt		Eg-Mwcnt	
		τ(1)	**Nu(1)**	**τ(1)**	**Nu(1)**
B	0.25	-0.502712	-0.184469	-0.502928	-0.405918
	0.5	-0.502709	-0.184467	-0.502921	-0.405907
	1.0	-0.502706	-0.184465	-0.502914	-0.404602
A11	0.1	-0.502712	-0.184469	-0.502928	-0.405918
	0.3	-0.502709	-0.182568	-0.502921	-0.401729
	0.5	-0.502706	-0.180666	-0.502914	-0.400246
B11	0.3	-0.502712	-0.184469	-0.502928	-0.405918
	0.5	-0.502709	-0.184467	-0.502921	-0.405907
	1.0	-0.502706	-0.184465	-0.502914	-0.405902
Rd	0.5	-0.502712	-0.184469	-0.502928	-0.405918
	1.5	-0.502714	-0.102477	-0.502929	-0.225483
	5.0	-0.502716	-0.040093	-0.502930	-0.088787
Ec	0.05	-0.502712	-0.184469	-0.502928	-0.405918
	0.1	-0.502706	-0.304786	-0.502914	-0.670669
	0.2	-0.502697	-0.425090	-0.502892	-0.943638
E1	0.3	-0.502712	-0.184468	-0.502928	-0.405917
	0.5	-0.502709	-0.184467	-0.502921	-0.405907
	0.7	-0.502706	-0.184465	-0.502914	-0.405615
δ	0.1	-0.502712	-0.184469	-0.502928	-0.405918
	0.2	-0.502709	-0.184467	-0.502921	-0.405907
	0.3	-0.502706	-0.184464	-0.502914	-0.405601
Q1	0.25	-0.507395	-1.900616	-0.507636	-0.418823
	0.5	-0.507013	-1.897487	-0.507626	-0.418455
	1.0	-0.506755	-1.792927	-0.507596	-0.418161
ε	0.1	-0.507736	-1.909656	-0.507636	-0.420294
	0.2	-0.507253	-1.907496	-0.507968	-0.420445
	0.3	-0.506987	-1.899256	-0.508168	-0.420799
β1	0.15	-0.507013	-1.902565	-0.507636	-0.419558
	0.25	-0.507223	-1.902495	-0.507639	-0.418664
	0.35	-0.507754	-1.902225	-0.507706	-0.417558

Table 6.2 : Skin friction(τ) & Nusselt number(Nu) with Swcnt-Eg and Mwcnt-Eg at r= 2

Paramater		Eg-Swcnt		Eg-Mwcnt	
		τ(2)	**Nu(2)**	**τ(2)**	**Nu(2)**
B	0.25	0.487243	0.181037	0.487019	0.398150
	0.5	0.487240	0.181034	0.487012	0.398139
	1.0	0.487237	0.181032	0.487005	0.317827
A11	0.1	0.487243	0.181037	0.487019	0.398150
	0.3	0.487240	0.179147	0.487012	0.393988
	0.5	0.487238	0.177258	0.487006	0.392526
B11	0.3	0.487243	0.181037	0.487019	0.398150
	0.5	0.487240	0.181034	0.487012	0.398139
	1.0	0.487237	0.181032	0.487005	0.397629
Rd	0.5	0.487243	0.181037	0.487019	0.398150
	1.5	0.487245	0.100571	0.487018	0.221169
	5.0	0.487254	0.094561	0.487011	0.112569
Ec	0.05	0.487243	0.181037	0.487019	0.398150
	0.1	0.487237	0.298431	0.487005	0.656288
	0.2	0.487229	0.415812	0.486984	0.922621
E1	0.3	0.487243	0.181036	0.487019	0.398149
	0.5	0.487240	0.181034	0.487012	0.398042
	0.7	0.487237	0.181031	0.487005	0.400843

Paramater		Eg-Swcnt		Eg-Mwcnt	
		τ(2)	Nu(2)	τ(2)	Nu(2)
δ	0.1	0.487243	0.181037	0.487019	0.398150
	0.2	0.487240	0.181034	0.487012	0.398739
	0.3	0.487237	0.181032	0.487005	0.400828
Q1	0.25	0.491809	1.86553	0.491599	0.410827
	0.5	0.492434	1.86478	0.491611	0.410478
	1.0	0.493258	1.86358	0.491629	0.410204
ε	0.1	0.492056	1.87381	0.491599	0.412191
	0.2	0.492609	1.87416	0.491848	0.412638
	0.3	0.491563	1.87528	0.491849	0.412768
β1	0.15	0.492434	1.86945	0.491599	0.411505
	0.25	0.492445	1.86941	0.491601	0.410669
	0.35	0.491259	1.86557	0.491921	0.410255

Table 6.3 : Sherwood number with Swcnt-Eg and Mwcnt-Eg at r=1 & 2

Parameter		Eg-Swcnt		Eg-Mwcnt	
		Sh(1)	Sh(2)	Sh(1)	Sh(2)
B	0.25	-0.895775	0.882346	-0.895351	0.881779
	0.5	-0.895763	0.882345	-0.895337	0.881766
	3	-0.895757	0.882334	-0.895314	0.881743
A11	0.1	-0.895775	0.882346	-0.895351	0.881779
	0.3	-0.895767	0.882344	-0.895346	0.881774
	0.5	-0.895759	0.882342	-0.895332	0.881766
B11	0.3	-0.895775	0.882346	-0.895351	0.881779
	0.5	-0.895763	0.882345	-0.895336	0.881765
	1	-0.895757	0.882333	-0.895312	0.881745
Rd	0.5	-0.895775	0.882346	-0.895351	0.881779
	1.5	-0.895947	0.882519	-0.895742	0.882161
	5	-0.896086	0.882655	-0.896047	0.882457
Ec	0.05	-0.895775	0.882346	-0.895351	0.881779
	0.1	-0.895494	0.882078	-0.894743	0.881189
	0.2	-0.895213	0.881804	-0.894097	0.880566
E1	0.2	-0.894109	0.880705	-0.893691	0.880139
	0.4	-0.897271	0.883829	-0.896843	0.883254
	0.6	-0.899875	0.886403	-0.899429	0.885808
δ	0.1	-0.895778	0.887346	-0.895351	0.881779
	0.3	-0.895763	0.882348	-0.895336	0.881765
	0.5	-0.895757	0.882333	-0.895315	0.881743
Q1	0.25	-0.010847	0.00730584	-0.0108481	0.00730524
	0.5	-0.0108485	0.00730984	-0.0108485	0.00730522
	1	-0.0108499	0.007311238	-0.0108489	0.00730519
ε	0.1	-0.0108547	0.00731066	-0.0108481	0.00730524
	0.2	-0.0108539	0.00731324	-0.0108556	0.00730993
	0.3	-0.0108522	0.00731948	-0.0108567	0.007322993
β1	0.15	-0.0108485	0.00730984	-0.0108481	0.00730524
	0.25	-0.0108489	0.00730994	-0.0108482	0.00730519
	0.35	-0.0108466	0.007312237	-0.0108489	0.00730512

7. CONCLUSIONS :

The non-linear, coupled equations governing the flow have been executed by numerical methods. From the variations of velocity, temperature and nanoconcentration with different parameters, we conclude that

- Increase in space and temperature dependent heat source parameters (A11, B11) / viscosity parameter (B) decays the velocity, temperature and nanoconcentration in the flow field in both types of nanofluid.
- Increase in Ec upsurges the temperature depreciates the velocity, nanoconcentration.
- Higher thermal radiation (Rd) larger velocity, nanoconcentration,depreaciates the temperature in the flow.
- Increase in Activation energy (E1) reduces velocity, temperature and enhances the nano-concentration.
- Increase in temperature difference ratio (δ) smaller the velocity, nanoconcentration while the temperature reduces in SWCNT case and enhances in MWCNT case.

REFERENCES:

1. Abbas SZ, Khan WA, Kadry S, Khan MI, Waqas M, Khan MI,(2020): Entropy optimized Darcy-Forchheimer nanofluid (silicon dioxide, molybdenum disulfide) subject to temperature dependent viscosity. *Comput Methods Progr Biomed*. 190:105363.
2. Abu-Nada Eiyad , Masoud Ziyad N., Hijazi Ala L,(2007): Natural Convection Heat Transfer Enhancement in Horizontal Concentric Annuli Using Nanofluids, May 2008, *International Communications in Heat and Mass Transfer* 35(5):657-665, DOI:10.1016/j.icheatmasstransfer. 11.004
3. Abu-Nada Eiyad,(2010): Effects of Variable Viscosity and Thermal Conductivity of CuO-Water Nanofluid on Heat Transfer Enhancement in Natural Convection: Mathematical Model and Simulation, *Journal of Heat Transfer* 132(5):052401, DOI:10.1115/1.4000440
4. Adebowale Martins Obalalu, Olusegun Adebayo Ajala, Adeshina Taofeeq Adeosun, Akintayo Oladimeji Akindele, Olayinka Akeem Oladapo, Olatunbosun Akintayo Olajide, Adegbite Peter,(2021): Significance of variable electrical conductivity on non-Newtonian fluid flow between two vertical plates in the coexistence of Arrhenius energy and exothermic chemical reaction, *Partial Differential Equations in Applied Mathematics*, 4, 100184, https://doi.org/10.1016/j.padiff.2021.100184
5. Adesanya SO, Falade JA, Ukaegbu JC, Makinde OD,(2016): Adomian-Hermite-Pade approximation approach to thermal criticality for a reactive third grade fluid flow through a porous medium. *Theor Appl Mech*. 43(1):pp.133–144.
6. Adeshina T. Adeosun, Joel C. Ukaegbu, (2022) Effect of the variable electrical conductivity on the thermal stability of the MHD reactive squeezed fluid flow through a channel by a spectral collocation Approach, *Partial Differential Equations in Applied Mathematics*, 5 ,100256, https://doi.org/ 10.1016/j.padiff.2021.100256
7. Al-Marri J., Ismail W. Almanassra , Ahmed Abdala , Muataz A. Atieh,(2016): Heat transfer enhancement of nanofluids using iron nanoparticles decorated carbon nanotubes, *Appl. Thermal Eng*. 107 (25) ,pp. 1008–1018.
8. Amitosh Tiwari (2013) : activation energy impacts on hydromagnetic convective heat transfer flow of nanofluid past a surface of vertical wavy with variable properties, *International Journal of Computer Applications (0975 – 8887)* (2023)*Volume 184 – No. 50,* www.ijcaonline.org
9. Arash Karimipour , Abdolmajid Taghipour , Amir Malvandi,(2016): Developing the laminar MHD forced convection flow of wa- ter/FMWNT carbon nanotubes in a microchannel imposed the uniform heat flux, *J. Magn. Magn. Mater*. 419 pp. 420–428 .
10. Berrehal H. and Maougal A,(2019):Entropy generation analysis for multi-walled carbon nanotube (MWCNT) suspended nanofluid flow over wedge with thermal radiation and convective boundary condition *Journal of Mechanical Science and Technology*, vol. 33, no. 1, pp. 459–464.
11. Buongiorne,J,(2006):Convective transport in Nanofluids, *Journal Heat transfer*128,pp.250-250.
12. Choi S.U.S and Eastman,A(1995) Enhancinh thermal conductivity of fluids with Nanoparticles, *ASME publications-Fed*. 231,pp.99-106
13. Choi SUS, Singer DA, Wang HP,(1995). Developments and applications of non-Newtonian flows. *ASME Fed.*;66:pp.99–105.
14. Devasena Y,(2023):Effect of non-linear thermal radiation, activation energy on hydromagnetic convective heat and mass transfer flow of nanofluid in vertical channel with Brownian motion and thermophoresis in the presence of irregular heat sources, *World Journal of Engineering Research and Technology* (JERT) *wjert, Vol. 9, Issue 2, XX-XX*, ISSN 2454-695X, SJIF Impact Factor: 5.924, www.wjert.org
15. Gopi P,(2024):Effect of heat generating sources on hydromagnetic convective heat transfer flow of rotating swcnt and mwcnt nanofluid in vertical channel with inconstant viscosity, *Journal of Engineering, Computing & Architecture*, Volume 14, Issue 01, pp.76-93, ISSN NO:1934-7197, http://www.journaleca.com/

16. Hayat T, Qayyum S, Alsaedi A,(2016): Thermally radiative stagnation point flow of maxwell nanofluid due to unsteady convectively heated stretched surface. *J Molecular Liquids*.;224:801–810.
17. Jewel Rana B. M., Raju Roy, Lasker Ershad Ali, Ahmmed S. F,(2017): Radiation Absorption and Variable Electrical Conductivity Effect on High Speed MHD Free Convective Flow past an Exponential Accelerated Inclined Plate, *World Journal of Mechanics*, 7, 211-241, DOI: 10.4236/wjm.2017.78019 http://www.scirp.org/journal/wjm, ISSN Online: 2160-0503, ISSN Print: 2160-049X
18. Kamali R, Binesh A ,(2010): Numerical investigation of heat transfer enhancement using carbon nanotube-based non-Newtonian nanofluids, *Int. Commun. Heat Mass Transf*. Vol.37(8), pp.1153–1157
19. Kathyani,G and Venkata Subrahmanyam,P,(2023):Effect of dissipation on HD convective heat and mass transfer flow of thermally radiating nanofluid in vertical channel with activation energy and irregular heat sources., *Mukth Shabd Journal(*Scientific Journal*)*, ISSN No.2347 -3150, ISSN No:2347-3150, Vol.XII,Issue.III, pp.433-441
20. Kiran Kumar T,Srinivasa Rao P, and MD. Shamshuddin,(2024): Effect of thermal radiation on nonDarcy hydromagnetic convective heat and mass transfer flow of a water-SWCNT's and MWCNT's nanofluids in a cylindrical annulus with thermo-diffusion and chemical n reaction. *International Journal of Modern Physics*. B, Vol. 38, No. 01, 2450011 (2024), https://doi.org/10.1142/ S0217979224500115.
21. Kumaresan V, Khader SMA, Karthikeyan S, Velraj (2013): Convective heat transfer characteristics of CNT nanofluids in a tubular heat exchanger of various lengths for energy efficient cooling/heating system. *International Journal of Heat and Mass Transfer*. ;60:pp.413-421
22. Lalramngaihzualí H. and Prasada Rao D.R.V,(2024): Numerical study of MHD convective heat transfer flow of Ethylene Glycol based SWCNT and MWCNT nanofluids in cylindrical annulus with variable viscosity, activation energy, *International Development international Journal of Novel Research and Development*, IJNRD | Volume 9, Issue 3, ISSN: 2456-4184, IJNRD.ORG
23. Lebelo RS, Mahlobo RK, Adesanya SO,(2019): Reactant consumption and thermal decomposition analysis in a two-step combustible slab. *Defect Diffus Forum*. 393:pp.59–72.
24. Makinde OD,(2012) Hermite-Pade approach to thermal stability of reacting masses in a slab with asymmetric convective cooling. *J Franklin Inst*. 349:pp.957–965.
25. Maria Imtiaz , Tasawar Hayat , Ahmed Alsaedi , Bashir Ahmad,(2016): Convective flow of carbon nanotubes between rotating stretch- able disks with thermal radiation effects, *Int. J. Heat Mass Transf.* 101,pp. 948–957.
26. Mehdi Nojoomizadeh , Arash Karimipour, (2016) : The effects of poros- ity and permeability on fluid flow and heat transfer of multi walled carbon nano-tubes suspended in oil (MWCNT/oil nano-fluid) in a microchannel filled with a porous medium, *Phys. E: Low-dimensional Syst. Nanostrut.* 84,pp. 423–433.
27. Nagasasikala M,(2023) :Effect of activation energy on convective heat and mass transfer flow of dissipative nanofluid in vertical channel with Brownian motion and thermophoresis in the presence of irregular heat sources, *World Journal of Engineering Research and Technology* (JERT) *wjert, , Vol. 9, Issue 2, XX-XX,* ISSN 2454-695X, SJIF Impact Factor: 5.924, www.wjert.org
28. Oztop H. F. and Abu-Nada E,(2008) "Numerical study of natural convection in partially heated rectangular enclosures filled with nanofluids," *International Journal of Heat and Fluid Flow*, vol. 29, no. 5, pp. 1326–1336.
29. Satya Narayana K and Ramakrishna G N,(2023) : Effect of variable viscosity, activation energy and irregular heat sources on convective heat and mass transfer flow of nanofluid in a channel with brownian motion and thermophoresis, *World Journal of Engineering Research and Technology* (WJERT), (2023), *Vol. 9, Issue 2, XX-XX,* ISSN 2454-695X, SJIF Impact Factor: 5.924, www.wjert.org
30. Shafiq A., Khan I., Rasool G., Sherif E. M., and Sheikh A. H,(2020):Influence of single- and multi-wall carbon nanotubes on magnetohydrodynamic stagnation point nanofluid flow over variable thicker surface with concave and convex effects, *Mathematics*, vol. 8, no. 104.
31. Shahsavar A., Saghafian M., Salimpour M.R., Shafii M.B,(2016): Experimental investigation on laminar forced convective heat transfer of ferrofluid loaded ith carbon nanotubes under con- stant and alternating magnetic fields, *Exp. Thermal Fluid Sci* 76,pp. 1–11.
32. Srijana Sharma and D.R.V.Prasada Rao,(2024):Finite element analysis of convective heat transfer flow of Ethylene Glycol based SWCNT and MWCNT rotating nanofluids in a vertical channel with variable viscosity, Activation energy,/heat generating sources and Hall effects., *Journal of Emerging Technologies and Innovative Research*., Vol.11,Issue.3,,pp.157-167.
33. Suvarna T,(2023):Finite element appoach of hydromagnetic heat and mass transfer flow of rotating fluid in a channel with activation energy: Presented in *International Conference On Innovations And Developments In*

Mathematical Sciences, And Technology (ICIDMST-2023), June 29th – 31st, Sri Krishnadevaraya University, A.P., India

34. Svante Arrhenius ,(2018):Activation Energy and the Arrhenius Equation – Introductory Chemistry- 1st Canadian Edition". opentextbc.ca. Archived from the original on 2017-07-08. Retrieved 2018-04-05.
35. Tao, L.N,(1960):On combined and forced convection in channels, *ASME J. Heat Transfer*, V.82, 233-238.
36. Tiwari R. K. and Das M. K,(2007):Heat transfer augmentation in a two-sided lid-driven differentially heated square cavity utilizing nanofluids, *International Journal of Heat and Mass Transfer*, vol. 50, no. 9-10, pp. 2002–2018.
37. Vijayalakshmi,P,(2021):Effect of thermal radiation on non-darcy hydromagnetic convective heat and mass transfer flow of water-swcnt's nanofluid in a cylindrical annulus with thermo-diffusion and chemical reaction, *Journal of Xi's University of Archetecture and Technology*, Issn No.1006-7930,V.Xiii,Issue.3,pp.16-29
38. Waqas M,(2019): Simulation of revised nanofluid model in the stagnation region of cross fluid by expanding-contracting cylinder. *Int J Numer Methods Heat Fluid Flow*. 30(4), pp. 2193-2205. https://doi.org/10.1108/HFF-12-2018-0797